User Manual: AO-qOCTA Method

Tool Reference

RST Reference Number: RST26OM05.01

Date of Publication: 05/21/2026

Recommended Citation: U.S. Food and Drug Administration. (2026). *A 3D Quantitative Optical Coherence Tomography Angiography Method for Measuring Retinal Blood Flow in Humans* (RST26OM05.01). https://cdrh-rst.fda.gov/3d-quantitative-optical-coherence-tomography-angiography-method-measuring-retinal-blood-flow-humans

For more information

Catalog of Regulatory Science Tools to Help Assess New Medical Devices

Disclaimer

About the Catalog of Regulatory Science Tools

The enclosed tool is part of the Catalog of Regulatory Science Tools, which provides a peer-reviewed resource for stakeholders to use where standards and qualified Medical Device Development Tools (MDDTs) do not yet exist. These tools do not replace FDA-recognized standards or MDDTs. This catalog collates a variety of regulatory science tools that the FDA's Center for Devices and Radiological Health's (CDRH) Office of Science and Engineering Labs (OSEL) developed. These tools use the most innovative science to support medical device development and patient access to safe and effective medical devices. If you are considering using a tool from this catalog in your marketing submissions, note that these tools have not been qualified as Medical Device Development Tools and the FDA has not evaluated the suitability of these tools within any specific context of use. You may request feedback or meetings for medical device submissions as part of the Q-Submission Program.

For more information about the Catalog of Regulatory Science Tools, email RST_CDRH@fda.hhs.gov.

RST Instruction Manual: AO-qOCTA Method

AO imaging system

The FDA Fourier-domain mode-locked (FDML) multimodal adaptive optics (AO) system has been described previously [1]. It includes optical coherence tomography (OCT) and scanning laser ophthalmoscope (SLO) channels, though the proposed method is based only on the AO-OCT mode in this study. The system features a 3.348 MHz FDML laser with a 1060 nm center wavelength and 76 nm bandwidth, providing 8.4 µm axial resolution in the eye (n=1.38). The sample arm has four pairs of reflective afocal telescopes conjugating the pupil to active components: a resonant scanner (3.270 kHz, 512 pixels) for fast scans, a galvanometer scanner for slow scans, a Shack-Hartmann wavefront sensor, and a deformable mirror. A superluminescent diode (850 nm) serves as the AO beacon. Interference signals are collected via a balanced detector and digitized. The system enables an OCT B-scan rate of 6.539 kHz and a maximum field of view (FOV) of 4.5°×4.5° (1.35 × 1.35 mm²) at the retina. Based on Rayleigh criterion, the AO-OCT beam achieves a 2.89 µm transverse resolution for an eye with a 16.7 mm axial length and 7.4 mm pupil diameter. An OLED micro display provides internal fixation across a 30° retinal region. Custom LabVIEW software manages system control, synchronization, real-time visualization, and data saving.

Human imaging protocol

Any human subject research testing should first be approved by an Institutional Review Board (IRB) and adhere to the tenets of the Declaration of Helsinki. Clinical measurements with FDA-approved devices do not require IRB approval. AO-SLO channel aids in the identification of region of interest with vasculature in the human retina prior to AO-OCT imaging but is not a pre-requisite. Vessels must meet the small angle criteria (~5° to 15°) with respect to the fast scan direction within the FOV. The shallow vessel angle requirement ensures that the angle of discrete streaks on the space-time images can be resolved resulting in a more reliable blood flow velocity quantitative analysis. Following are important steps for human imaging:

- The volunteer's pupil should be dilated for AO imaging (e.g., with 1% tropicamide).
- The AO-OCT channel should be operated in OCTA mode with selected repeat B-scans, as shown in **Fig. 1**. For method demonstration, we operated with an eight repeat B-scans (4 forward and 4 backward) per slow scan position.
- For method demonstration, at the identified region of interest, a FOV of 1.5°×1.5° in OCTA mode (1.6 vol/s, 512×512 pixels) was used, though other FOVs can be used, depending on vessel size.
- System focus was set by the deformable mirror to the superficial vascular plexus in the inner retina.
- In AO-OCTA mode, collect a single OCTA volume. It may be necessary to collect multiple sequential OCTA volumes to capture multiple cardiac cycles.

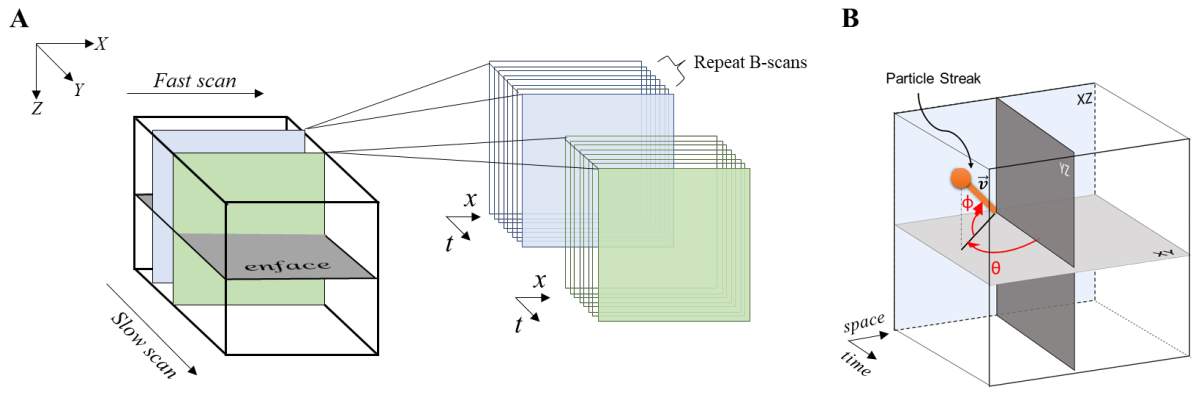

Fig. 1A. Illustrates acquisition of sequences of repeat two-dimensional B-scans associated with a fast scan direction at different slow scan positions. **B.** Each space time slice captures a streak associated with a moving blood cell whose projections on XY and YZ planes produce spatio-temporal images.

Post-processing method

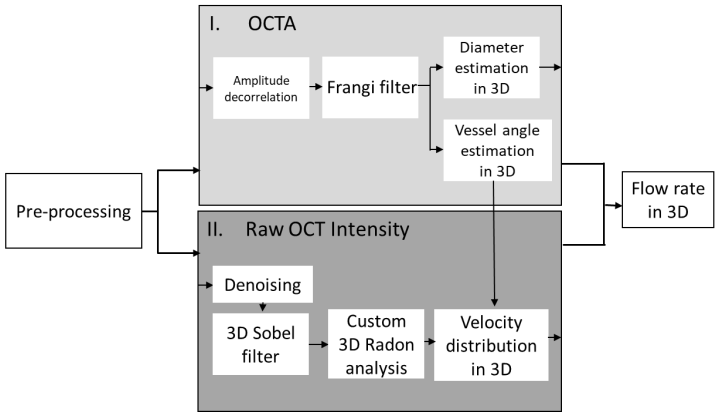

Fig. 2. Illustrates post-processing pipeline to determine voxel wise 3D velocity and flow rates.

The AO-qOCTA method [2] includes two key sub-processing pipelines that can be run in parallel, as illustrated in the **Fig. 2**. Axial eye lengths are measured during the clinical exam and used to correct retina magnification factor according to the method introduced by Bennett et al. [3]. The two key measures for calculating 3D blood flow rate are vessel diameter and flow velocity at each voxel, both derived from same AO-OCT volume analysis, as outlined below.

i. OCTA analysis for morphology

1. The reconstructed raw OCT volume is processed for 3D visualization of vasculature. Among many methods for OCTA analysis, a amplitude decorrelation approach was used to demonstrate the OCTA signal calculation from the spatio-temporal OCT scans for visualizing and extracting morphological characteristics of the retinal vessels [4].
2. Bulk target motion induced artifact is negligible owing to high B-scan rate (> 1000 fps).
3. Before the morphological features extraction step, Hessian-based Frangi vesselness filter is applied on 3D OCTA image which allows enhancement of tubelike structures and suppression of non-tubular structures and background noise [5].

4. Morphological features such as vessel diameter and orientation in 3D could be extracted with built in MATLAB functions.

ii. Raw OCT intensity analysis for velocity

1. The raw AO-OCT volume containing streaks is denoised to reduce speckle noise using shearlet domain thresholding. Since the shearlet transform often assumes that the underlying noise follows a Gaussian distribution, a square root transformation was first applied to the pre-processed spatio-temporal OCT volume before 3D shearlet transformation [6].
2. A fixed threshold was applied on the computed 3D shearlet coefficients as described by Yang, et. al. [7].
3. Further, application of a Sobel filter removes the static features which appear as bright vertical lines in the pre-processed volume.
4. To automatically quantify streak orientation in spatio-temporal volume a custom 3D Radon algorithm is implemented similar to existing 2D Radon algorithm detailed elsewhere [8, 9].
5. For computing absolute particle velocity, knowledge of the vessel orientation to the fast axis scan direction is required. This is derived from the segmented OCTA image by calculating the local gradient of the vessel centerline. Particle velocity can be calculated with the equation:

$$v_{particle} = \sqrt{(f * \cot\theta * sec\chi)^2{}_{XY} + (f * \cot\varphi * sec\chi)^2{}_{YZ}}$$

where, $v_{particle}$ is the local individual particle velocity (mm/s), f is equal to the B-scan rate (Hz) multiplied by sampling density (µm/pixel) and χ is the vessel orientation to the fast axis.

By combining velocity and diameter measurements, 3D flow rates are mapped under the assumption of a circular cross-sectional area for the retinal vessels. The complete post-processing and visualization pipeline was developed in MATLAB. The described method allows, for example, distinguishing blood vessel types based on streak orientation (**Fig. 3A**). Furthermore, the flow rates can be visualized along with overlapping vasculature, including parabolic variation within each vessel, as shown in **Fig. 3B**.

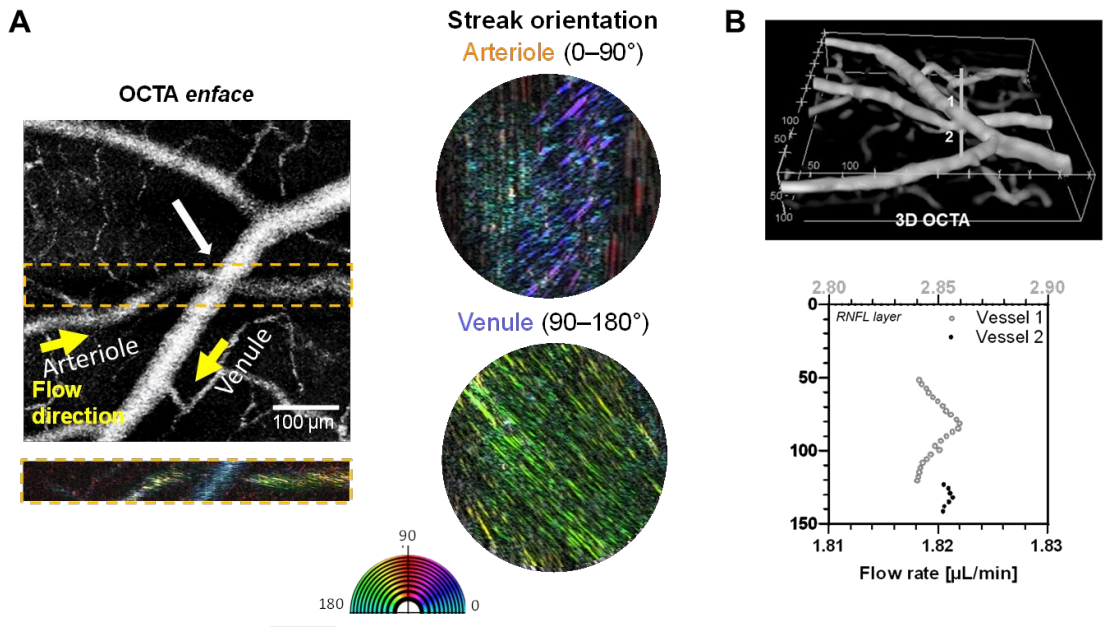

Fig. 3A. Illustrates the ability to determine blood vessel type based on the observed streak orientation and **B.** to discriminate and quantify parabolic flow rate of overlapping vessels in depth which can obtained with the described method.

References

1. Z. Liu, *et al.*, "Ultrahigh-speed multimodal adaptive optics system for microscopic structural and functional imaging of the human retina," Biomedical Optics Express **13**, 5860-5878 (2022).
2. A. J. Raghavendra, *et al.*, "Single-scan adaptive optics-enabled quantitative optical coherence tomography angiography for absolute three-dimensional retinal blood flow mapping," Optica **13**, 125-134 (2026).
3. A. G. Bennett, *et al.*, "Improvements on Littmann's method of determining the size of retinal features by fundus photography," Graefe's archive for clinical and experimental ophthalmology **232**, 361-367 (1994).
4. Y. Jia, *et al.*, "Split-spectrum amplitude-decorrelation angiography with optical coherence tomography," Optics express **20**, 4710-4725 (2012).
5. R. K. Meleppat, *et al.*, "Multiscale Hessian filtering for enhancement of OCT angiography images," in *Ophthalmic technologies XXIX*(SPIE2019), pp. 64-70.
6. W.-Q. Lim, "The discrete shearlet transform: A new directional transform and compactly supported shearlet frames," IEEE Transactions on image processing **19**, 1166-1180 (2010).
7. J. Yang, *et al.*, "Universal digital filtering for denoising volumetric retinal OCT and OCT angiography in 3D shearlet domain," Optics Letters **45**, 694-697 (2020).
8. A. Joseph, *et al.*, "Imaging single-cell blood flow in the smallest to largest vessels in the living retina," elife **8**, e45077 (2019).
9. P. J. Drew, *et al.*, "Rapid determination of particle velocity from space-time images using the Radon transform," Journal of computational neuroscience **29**, 5-11 (2010).